



**HAL**  
open science

# Estimation and prediction of vehicle dynamics states based on fusion of OpenStreetMap and vehicle dynamics models

Kun Jiang, Alessandro Corrêa Victorino, Ali Charara

## ► To cite this version:

Kun Jiang, Alessandro Corrêa Victorino, Ali Charara. Estimation and prediction of vehicle dynamics states based on fusion of OpenStreetMap and vehicle dynamics models. IEEE Intelligent Vehicles Symposium (IV 2016), Jun 2016, Göteborg, Sweden. pp.208-213. hal-01310763

**HAL Id: hal-01310763**

**<https://hal.science/hal-01310763>**

Submitted on 3 May 2016

**HAL** is a multi-disciplinary open access archive for the deposit and dissemination of scientific research documents, whether they are published or not. The documents may come from teaching and research institutions in France or abroad, or from public or private research centers.

L'archive ouverte pluridisciplinaire **HAL**, est destinée au dépôt et à la diffusion de documents scientifiques de niveau recherche, publiés ou non, émanant des établissements d'enseignement et de recherche français ou étrangers, des laboratoires publics ou privés.



proposed to predict the vehicle rollover phenomenon of light all terrain vehicles. Some other vehicle rollover prediction method can be equally found in [12] for heavy vehicles. [13] proposes a algorithm for the curve speed prediction which addresses control loss due to excessive speed in curves. [10] proposes a vehicle full-state estimation system to describe overall vehicle dynamics.

The main contribution of this paper is to incorporate the digital-map and inertial sensors to estimate and predict the safety of vehicle. The method of how to get the road information through OSM is presented in Section II. Then section III describes the vehicle dynamics models and the risk assessment index. In Section IV, the whole estimation algorithm is presented. The results of experimental validation is illustrated in Section V. Finally, concluding remarks and future perspectives are given in Section VI.

## II. ROAD GEOMETRY ESTIMATION

OSM is a platform capable of describing a variety of information about roads. Typically, the OSM data is stored in a xml file. The OSM data model consists of three basic geometric elements: 1, *Node*, which defines points in space. Each node comprises at least an id number and a pair of coordinates. 2, *Way*, which represents linear features and area boundaries and is defined by an ordered list of nodes. 3, *Relation*, which is used to explain how other elements work together. Each element can be attributed to multiple tags to represent different road information.

### A. Road geometry description

The first problem we encountered is how to describe the road geometry with OSM. Note that the original database of OpenStreetMap doesn't contain the accurate information we need (curvature, friction, etc). Therefore, we created new database with our own measurement. In OSM, a road is represented by intensive and consecutive way points. It is unpractical to attribute geometry information to each point, due to the huge amount of work needed. In the publication of Victorino et al. [5], a topological representation of the robot path is proposed. Inspired by this work, the vehicle path in this paper is represented by corridors and the nodes of their intersections. The nodes of intersections were called as Critical Points (CP). The corridors are the roads between two CPs, without any other direction to go. The CPs are the locations where the vehicle dynamics states will change a lot (roundabout, slippery region or traffic light stop). Comparison with way points, the CPs can be defined sparsely and are attributed with many properties to describe the geometry of nearby road. The list of tags we attributed to each CP is illustrated in the Table 1.

Then the corridors can be obtained by connecting two CPs, as illustrated in Table 2. It is noted that the connections between two CPs can be straight lines or curves. In order to simplify the representation of corridor, the CPs should be selected carefully and the following assumption is made.

- Hypothesis 1: The CPs are pre-calculated so that each corridor is represented by a straight line or a clothoid;

TABLE I  
TAGS ATTRIBUTED TO CRITICAL POINTS

Longitude Position	Latitude Position	Altitude
$x$	$y$	$h$
Road Direction	Curvature	Concavity
$\psi_r$	$\kappa$	$\rho$
Road Friction	Bank Angle	Slope Angle
$\mu$	$\varphi$	$\theta$
ID in OSM	Number of lanes	Number of roads
$I_{dosm}$	$N_{lane}$	$N_{road}$

TABLE II  
TAGS ATTRIBUTED TO CORRIDORS

Id of Beginning CP	Id of Ending CP	Length of Corridor
$I_{d_0}$	$I_{d_n}$	$L_{corr}$
Id of corridor	Curve or Line	Stop or Not
$I_{d_{way}}$	$R_{curve} = \{0, 1\}$	$R_{stop} = \{0, 1\}$

- Hypothesis 2: The length of each corridor is known;
- Hypothesis 3: The change rates of road friction and road inclination angle can be approximately regarded as constant in each corridor.

The road geometry information vector listed in Table 1 is noted as  $State = [x y h \mu \kappa \theta \varphi x \rho \psi_r]$ . Based on Hypothesis 3, when the corridor is a straight road, the properties of each point in the straight corridor can be easily obtained by the Equation (1).

$$State_{current} = (1 - \frac{L}{L_{corr}})State_{CP_0} + \frac{L}{L_{corr}}State_{CP_n} \quad (1)$$

where the index "current" means the geometry of current point, "CP<sub>0</sub>" represents the beginning point of the corridor and "CP<sub>n</sub>" corresponds to the ending point,  $L$  is the distance between the current position and CP<sub>0</sub>.

When the corridor is a curve, the properties of a CP in a curve corridor can be also obtained by Equation (1), except for the position. According to the fundamentals of road design[4], the clothoid is widely used for urban road construction. They are defined by their begin curvature  $\kappa_0$  and a constant curvature change rate  $\kappa_1$  and their total length  $l$ . The current curvature of a clothoid after length  $l_c$  can be obtained by Equation (2).

$$\kappa(l_c) = \kappa_0 + \kappa_1 \cdot l_c \quad (2)$$

The variation of tangent angle after length  $l_c$  can be computed by integration of Equation (2) over  $l_c$ .

$$\Delta\psi = \frac{\kappa_0 + \kappa(l_c)}{2} l_c \quad (3)$$

The position of a point  $[x, y]^T$  in a curve corridor is given as Equation (4).

$$\begin{bmatrix} x \\ y \end{bmatrix} = \begin{bmatrix} x \\ y \end{bmatrix}_{CP_0} + \frac{2l_c}{\Delta\psi} \sin \frac{\Delta\psi}{2} \begin{bmatrix} \cos(\psi + \frac{1}{2}\Delta\psi) \\ \sin(\psi + \frac{1}{2}\Delta\psi) \end{bmatrix} \quad (4)$$

## B. Vehicle localization

The vehicle location is measured by a differential GPS sensor. However, the GPS has the problem of signal lost. Therefore, the Kalman filter algorithm is employed to combine the direct measurement and the integration of speed. As the kinematic model is non-linear, an Extended Kalman filter is applied to minimize the estimation errors. The continuous state equations and measurement models are given by Equation (5).

$$\begin{bmatrix} \dot{X} \\ \dot{Y} \\ \dot{v}_x \\ \dot{\psi} \\ \dot{\psi} \end{bmatrix} = \begin{bmatrix} \sin(\psi) \cdot v_x \\ \cos(\psi) \cdot v_x \\ a_x - g \sin \theta \\ \dot{\psi} \\ 0 \end{bmatrix} + noise \quad (5)$$

$$\begin{bmatrix} X_{gps} \\ Y_{gps} \\ v_{gps} \\ \psi_{gps} \\ v_{wheel} \\ \psi_{gyro} \end{bmatrix} = \begin{bmatrix} 1 & 0 & 0 & 0 & 0 \\ 0 & 1 & 0 & 0 & 0 \\ 0 & 0 & 1 & 0 & 0 \\ 0 & 0 & 0 & 1 & 0 \\ 0 & 0 & 1 & 0 & 0 \\ 0 & 0 & 0 & 0 & 1 \end{bmatrix} \begin{bmatrix} X \\ Y \\ v_x \\ \psi \\ \dot{\psi} \end{bmatrix} + noise$$

where  $X_{gps}$ ,  $Y_{gps}$ ,  $v_{gps}$ ,  $v_{wheel}$ ,  $\psi_{gps}$ ,  $\psi_{gyro}$  are the measurement of GPS receiver and inertial units,  $\psi$  is the clockwise angle between the north and the vehicle direction. In this equation, we suppose the lateral speed is negligible in the calculation of displacement.

The estimated vehicle location is used to identify the corresponding point in the OSM. The searching process can be divided into two steps: firstly searching for the corresponding corridor and secondly locating the relative position in the corridor. Supposing the initial position is already known, the total distance ( $l_{total}$ ) between current position and initial position is the sum of length of the passed corridors. Then the criterion for matching the corridor of number  $n$  is given by Equation (6).

$$\sum_{i=1}^{n-1} L_{corr,i} < l_{total} < \sum_{i=1}^n L_{corr,i} \quad (6)$$

$$l_{total,t} = l_{total,t-1} + v_x \cdot \Delta t$$

After the current corridor is identified, the vehicle position can be calculated with the two CPs of the corridor, as shown by Equation (1) or (4) depending on the corridor is straight or curve. As a result, we have two additional measurement about the location which could be used to improve the Kalman filter in Equation (5).

$$\begin{bmatrix} X_{osm} \\ Y_{osm} \end{bmatrix} = \begin{bmatrix} 1 & 0 & 0 & 0 & 0 \\ 0 & 1 & 0 & 0 & 0 \end{bmatrix} \begin{bmatrix} X \\ Y \\ v_x \\ \psi \\ \dot{\psi} \end{bmatrix} + noise \quad (7)$$

To eliminate the accumulated errors in the calculation of  $l_{total}$ , when the vehicle passed the ending point of the  $N$ th corridor, the  $l_{total}$  will be calibrated by Equation (8).

$$l_{total} = \sum_{i=1}^n L_{corr,i} \quad (8)$$

## III. DIAGNOSIS OF VEHICLE DYNAMIC BEHAVIORS

### A. Evaluation of safety

In order to evaluate vehicle's safety, we employ three risk assessment indexes: load transfer ratio ( $LTR$ ) and lateral skid ratio ( $LSR$ ), and the stopping distance ( $SD$ )[12]. The lateral load transfer ratio  $LTR$  is defined by using four wheel vertical forces as in Equation (9). The estimation method of vertical forces at each tire is introduced in our previous work [10].

$$LTR = \frac{F_{z11} - F_{z12} + F_{z21} - F_{z22}}{F_{z11} + F_{z12} + F_{z21} + F_{z22}} \quad (9)$$

The lateral skid ratio  $LSR$  represents the loss of adhesion resulting in the lateral drift. The lateral skid ratio is defined by road friction coefficient and tire forces, as in Equation (10). The estimation of lateral tire forces and slip angle is introduced in next subsection. The  $\mu_{max}$  is the threshold of safe friction, it should be smaller than the real friction coefficient.

$$LSR_{ij} = 1 - \frac{\mu_{max} - \mu_{ij}}{\mu_{max}} \quad (10)$$

$$\mu_{ij} = \frac{F_{yij}}{F_{zij}}$$

The stopping distance ( $SD$ ) refers to the distance needed to stop the vehicle. We assume that during the stopping process, the braking acceleration is a constant value  $a_{xmax}$ . The  $a_{xmax}$  is defined as to ensure the comfort of passengers. The stopping distance can be obtained by Equation (11).

$$SD = \frac{1}{2a_{xmax}} v_x^2 \quad (11)$$

### B. Vehicle dynamics models

The yaw rate, steering angle and accelerations are important parameters for vehicle dynamics estimation. In the literature, all these parameters are usually measured by inertial sensors. However, the unpredictable sensor failure may happen during driving. In this paper, we propose to employ data from digital map to provide redundant information about these basic dynamics parameters. Supposing that the vehicle successfully followed the the road curve, these vehicle dynamics parameters can be approximated by applying the kinematic relationship, as shown in Equation (12). The errors caused by the lane changing behavior can be viewed as the noises in the curvature  $\kappa_{osm}$ .

$$\begin{aligned} ax_{osm} &= dv_x/dt + g \sin \theta_{osm} \\ ay_{osm} &= v_x^2 \kappa_{osm} + g \sin \varphi_{osm} \\ az_{osm} &= v_x^2 \rho_{osm} + g \cos \theta_{osm} \cos \varphi_{osm} \\ \dot{\psi}_{osm} &= v_x \kappa_{osm} \\ \delta_{osm} &= L_v \kappa_{osm} \end{aligned} \quad (12)$$

where  $\theta_{osm}$  and  $\varphi_{osm}$  are the slope and bank angle of the road,  $\rho_{osm}$  is the vertical curvature of the road,  $\kappa_{osm}$  is the planar curvature, their value are obtained by Equation (1). When the  $\kappa_{osm}$  is the curvature at current point, Equation (12) can be regarded as an redundant resource of current dynamics states. While  $\kappa_{osm}$  is the curvature at future point, the computed accelerations and yaw rates can be employed to predict future dynamics states. The variance of  $\kappa_{osm}$  is set as  $0.03^2$ .

To simplify the estimation, the linear tire model and bicycle model are used to estimate the sideslip angle, as

shown in Equation (13). With this observer, we can also obtain the lateral force per axle. To obtain the lateral force at each tire, the double track model and Dugoff model are employed, as explained in our previous work [6,10].

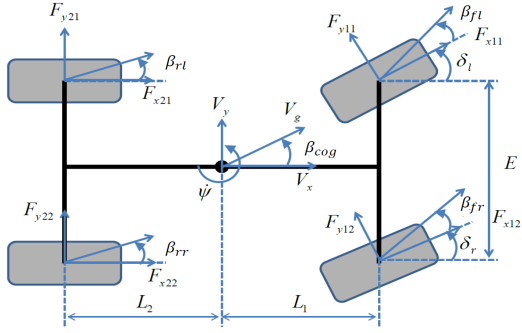


Fig. 3. Double track model

$$\begin{aligned}
 & [\ddot{\psi} \quad \dot{\beta}_{cog} \quad F_{xf} \quad F_{yf} \quad F_{yr}]^T = \\
 & \begin{bmatrix} -\frac{L_1^2 C_f + L_2^2 C_r}{I_z v_x} & \frac{L_2 C_r - L_1 C_f}{I_z} & 0 & 0 & 0 \\ -1 + \frac{L_2 C_r - L_1 C_f}{m_v v_x^2} & -\frac{C_f + C_r}{m_v v_x} & 0 & 0 & 0 \end{bmatrix} \begin{bmatrix} \dot{\psi} \\ \beta_{cog} \\ F_{xf} \\ F_{yf} \\ F_{yr} \end{bmatrix} \\
 & + \begin{bmatrix} \frac{L_1 C_f}{I_z} \\ \frac{C_f}{m_v v_x} \end{bmatrix} \delta + cov(noise) \\
 & \begin{bmatrix} \ddot{\psi} I_z \\ m_v a_y \\ m_v a_x \\ 0 \end{bmatrix} = \begin{bmatrix} L_1 \sin \delta & L_1 \cos \delta & -L_2 & 0 & 0 \\ \sin \delta & \cos \delta & 1 & 0 & 0 \\ \cos \delta & \sin \delta & 0 & 0 & 0 \\ \frac{L_2}{v_x} & -1 & 0 & 0 & \frac{1}{C_r} \end{bmatrix} \begin{bmatrix} \dot{\psi} \\ \beta_{cog} \\ F_{xf} \\ F_{yf} \\ F_{yr} \end{bmatrix} \\
 & + cov(noise) \tag{13}
 \end{aligned}$$

where  $C_f$ ,  $C_r$  are side slip stiffness of front tires and rear tires.  $L_1$ ,  $L_2$  are the distances from COG to front and rear axle.  $\delta$  is steering angle.  $I_z$  is vehicle yaw inertia.  $F_{yf}$  and  $F_{yr}$  are lateral forces at front and rear axle respectively,  $F_{xf}$  is the longitudinal tire forces at front axle.

#### IV. PREDICTION ALGORITHM

The overall prediction process can be expressed by the Figure 4. The sensor measurement is used to locate the vehicle's position and identify the corresponding corridors and CPs. Then CPs can provide information about road friction coefficient which can greatly improve the the estimation of current states. Moreover, by extracting the upcoming CPs, the estimator could predict the potential variation of dynamics states. Then the dynamics states of current instant and future instant will be evaluated by three indicators of safety, introduced in the above section. To simplify the prediction process, the vehicle speed is regarded as constant and equals to the current speed during the preview time. The prediction system will perform the risk assessment for the coming 300m road. If a potential danger is detected, the system will warn the driver to slow down. The predicted dynamics states can

also be used to control the stabilization system. However, in order to improve the accuracy of prediction, a more accurate model about the variation of speed is needed.

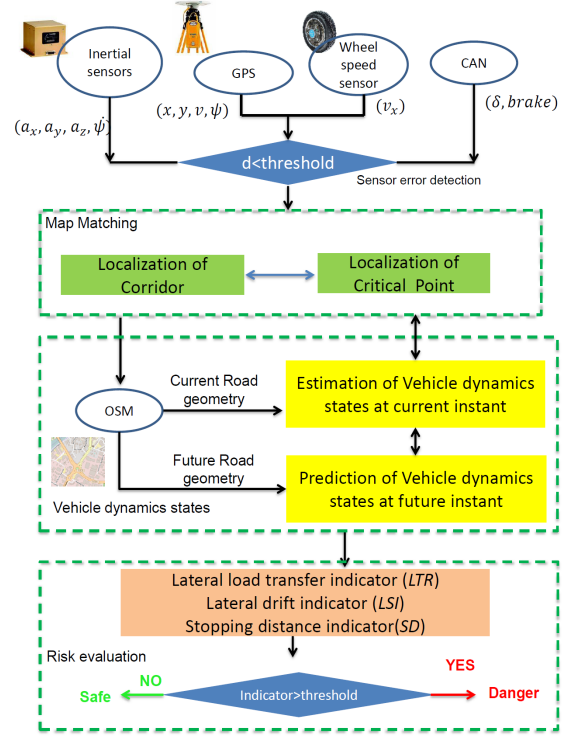


Fig. 4. Overall structure of vehicle safety prediction system

Due to the non-linearity of vehicle dynamics models, an extended Kalman filter (EKF) is used to minimize the estimation errors. The algorithm of EKF is shown in the Figure 5.

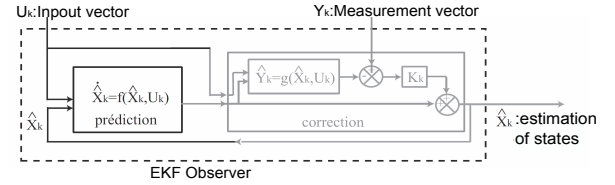


Fig. 5. Algorithm of Extended Kalman Filter

Sensor based measurement and map geometry based prediction provides two independent approaches for the observation of the vehicle dynamics. The Kalman filter algorithm could combine the two observation to minimize the variance of final estimation result.

#### V. EXPERIMENTAL VALIDATION

The experimental vehicle DYNA is instrumented by our laboratory, as shown in Figure 6. This experimental platform is dedicated to validate the algorithm of estimating vehicle dynamics. The details about these sensors are introduced in our previous work [6,10]. A remarkable point about our vehicle DYNA is the ability to directly measure the vertical and lateral tire forces, which were used as the ground truth to

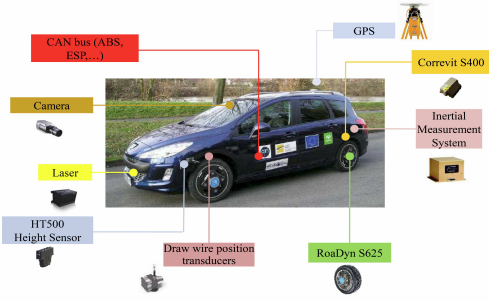


Fig. 6. Experimental vehicle: DYNA

validate the estimation results. The observers were validated in an off-line algorithm. The trajectory of the vehicle during the test is illustrated in Figure 7. In total, 53 critical points and 52 corridors were defined to describe the trajectory. More CPs were defined around the sharp turning and lane changing point in order to better describe the road. Some examples of CPs and corridors are demonstrated in Table 3. A segmentation of data ( $150 < t < 200s$ ) is selected due to the successive turning behaviors in this period. The maneuver time history are presented by red lines in Figure 8. The average speed is about 50 km/h.

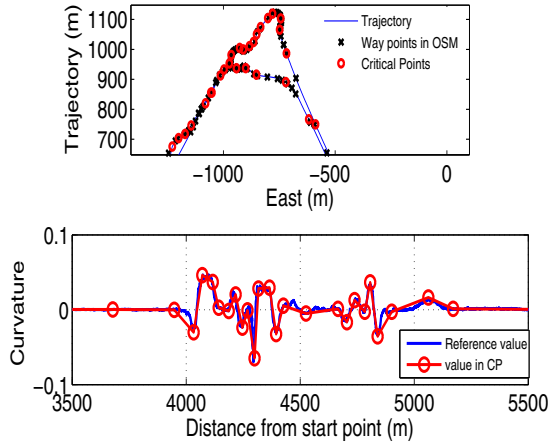


Fig. 7. Vehicle's trajectory and curvature value at each critical point

The curvature at each critical point is illustrated by red spots in Figure 7. The curvature between two critical points were computed by Equation (1), which is a linear interpolation of the two neighboring critical points. As we can see in Figure 7, the interpolation method (represented by red lines) was a simplification of real road geometry and was not always accurate. However, it effectively represented the main characteristic of the road. Then the obtained curvature was used to compute the value of accelerations and yaw rate with Equation (12). The comparison between inertial sensor measurement and digital map based (OSM) estimation was illustrated in Figure 8. Then two data are incorporated to provide a robust estimation about the basic dynamics parameters, as represented by green lines.

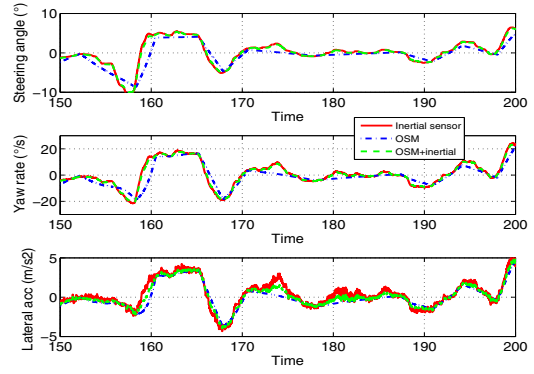


Fig. 8. Comparison of lateral dynamics states estimated by inertial sensors and OSM

The estimation results of tire forces are compared with the measurement of force transducer in Figure 9. The red lines are the measurement data. The green lines represented the estimation result based on inertial sensors. The blue lines corresponded to the estimation result based on the OpenStreetMap. The accuracy of the OSM method depends on the intensity of critical points and map quality. Moreover, it is also based on the assumption that the vehicle successfully followed the planned path. At  $t = 175s$ , the driver did a lane changing behavior, which was not in the planning and caused some errors. As demonstrated by the experimental result, the inertial sensor based method can better follow the vertical force variation, while, the OSM based estimation method is accurate when the vehicle is following the curve. Fusion of these two estimation provides a better estimation of vertical force, as expressed by solid black lines in the Figure 9.a). The similar situation can be found in the estimation of lateral force. Note that the shift in the estimation of  $F_y$  at front tires is caused by the Ackermann steering geometry. The steering angles at left tire and right tire are different, while we regarded as identical in this paper. The advantage of OSM is obvious in the estimation of sideslip angle. We configured the slip stiffness  $C_r$  as two times of the correct value. Therefore, the estimated sideslip angle is obvious smaller than measurement. The OSM method could get the correct  $C_r$  from the digital map, as we suppose  $C_r \propto \mu$ . It is clear that the combined method provided a better estimation of sideslip angle. Note that due to the position of the optic sensor, the direct measurement is actually the sideslip angle at rear axle  $\beta_r$ . The transformation between  $\beta_r$  and  $\beta_{cog}$  is given by  $\beta_{cog} = \beta_r + \frac{L_2 \dot{\psi}}{v_x}$ .

The curvature at each point is a function of the traveled distance, as shown in Figure 7. Then it is able to predict the curvature of following 300 meters ahead of the vehicle's current position. The vehicle's safety could be evaluated with the index introduced by Equation (9, 10, 11). Figure 10 illustrated the prediction of vehicle's safety situation in the following 300 meters at instant  $t = 160s$  and  $t = 180s$ . The results showed at instant  $t=180s$ , the algorithm detected potential dangers in the upcoming path.

CP ID	$x(m)$	$y(m)$	$h(m)$	$\psi_r(^{\circ})$	$\kappa$	$\rho$	$\mu_{max}$	$\varphi(^{\circ})$	$\theta(^{\circ})$	Corridor Id	$Id_0$	$Id_n$	$L_{corr}(m)$	$R_{curve}$	$R_{stop}$
7	-717.7	986.7	52.6	333.3	0	0	1	0	5	5	6	690	0	0	
8	-748.1	1066.1	56.8	2.1	-0.031	0	1	0	0	6	7	270	0	0	
9	-743.6	1103.3	57.0	343.7	0.046	0	1	0	0	7	8	85	1	1	

TABLE III  
THE CONSTRUCTION OF CRITICAL POINTS AND CORRIDORS

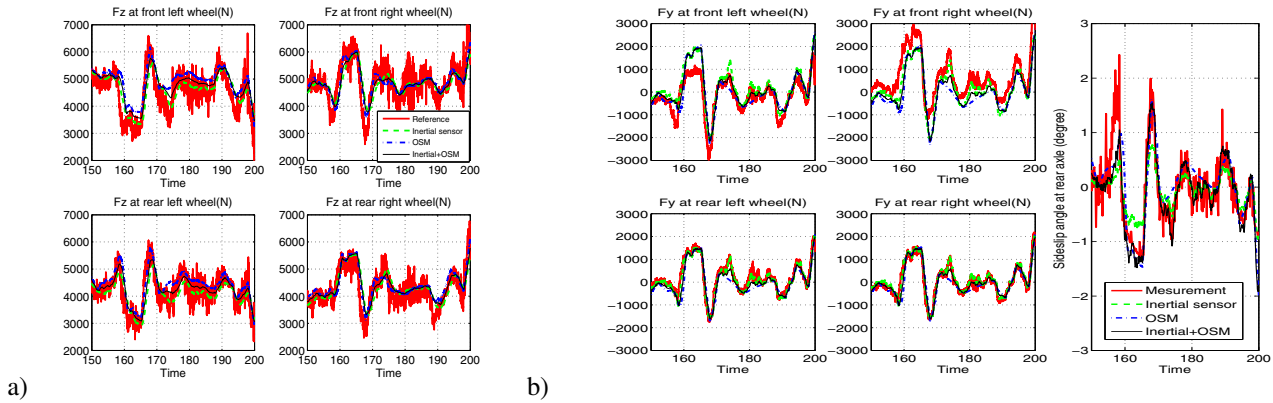


Fig. 9. a) Estimation of vertical forces at each tire; b) Estimation of lateral forces at each tire: comparison between sensor measurement and estimation

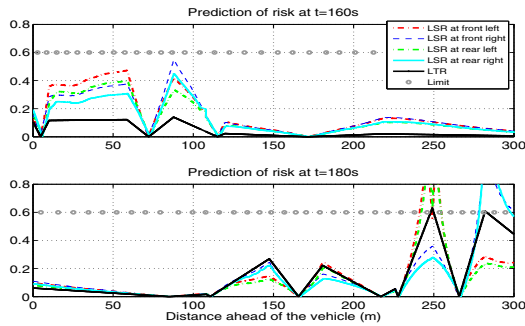


Fig. 10. Prediction of vehicle safety in the following 300 meters road

## VI. CONCLUSIONS AND PROSPECTS

This paper presented a novel method to estimate and predict vehicle dynamic states based on the fusion of OpenStreetMap and inertial sensors. The current and future road information was obtained from the digital map after the localization process. Then the vehicles models and map data are combined to evaluate the safety of the vehicle. Experimental results validated the proposed algorithm. The future work will focus on the improvement of map quality and localization accuracy.

## REFERENCES

- [1] A. Schindler, "Vehicle self-localization with high-precision digital maps," in Intelligent Vehicles Symposium, 2013 IEEE, June 2013, pp. 141-146.
- [2] M. Hentschel, B. Wagner, "Autonomous robot navigation based on openstreetmap geodata," in Intelligent Transportation Systems, 2010 13th International IEEE Conference on, Sept 2010, pp. 1645-1650.
- [3] R. Ghandour, F. Da Cunha, A. Victorino, A. Charara et D. Lechner, "A method of vehicle dynamics prediction to anticipate the risk of future accidents : Experimental validation", 14th Int. IEEE Conference on Intelligent Transportation Systems, Washington, USA, October 2011.
- [4] W. Kühn. Fundamentals of Road Design. WIT Press, 2013.
- [5] A. Victorino, et al. "Safe navigation for indoor mobile robots, partii: Exploration, self-localization and map building", International Journal of Robotics Research, vol. 22, no. 12, pp. 1019-1041, 2003.
- [6] B. Wang, Q. Cheng, et al. "Real-Time Experimental Validation of Nonlinear Observer for Vehicle Dynamics Parameters Estimation : A Laboratory Vehicle Description", 2012 IEEE Conference on Vehicular Electronics and Safety, Turkey, Jul, 2012
- [7] B. C. Chen and F. C. Hsieh, "Sideslip angle estimation using extended Kalman filter", Vehicle System Dynamics, vol. 46: S1, pp. 353-364, 2009.
- [8] G. Dherbomez, T. Monglon, P. Crubillé, B. Wang, A. C. Victorino et al. DYNA, véhicule expérimental pour la Dynamique du Véhicule. Quatrièmes Journées des Démonstrateurs en Automatique, 2013.
- [9] Cejun Liu, Ph.D, and Tony Jianqiang Ye. "Run-Off-Road Crashes: An On-Scene Perspective". (2011) DOT HS 811 500. Washington, DC: National Highway Traffic Safety Administration.
- [10] K. Jiang, A.C. Victorino, et A. Charara. Adaptive estimation of vehicle dynamics through RLS and Kalman filter approaches. Intelligent Transportation Systems, 2015 IEEE 18th International Conference on. IEEE, 2015. p. 1741-1746.
- [11] N. Bouton, R. Lenain, B. Thuilot and J. C. Fauroux. "A rollover indicator based on the prediction of the load transfer in presence of sliding: application to an All Terrain Vehicle". In 2007 IEEE Int. Conference on Robotics and Automation, pages 1158-1163, 2007.
- [12] H. Imine and V. Dolcemascolo. "Rollover risk prediction of heavy vehicle in interaction with infrastructure". International Journal of Heavy Vehicle Systems, vol. 14, no. 3, pages 294-307, 2007.
- [13] C. Sentouh, S. Glaser and S. Mammari. "Advanced vehicle infrastructure- driver speed profile for road departure accident prevention". Vehicle System Dynamics, vol. 44, pages 612-623, 2006.